Precision microwave electrodynamic measurements of K- and Co-doped BaFe₂As₂

J. S. Bobowski, J. C. Baglo, James Day, P. Dosanjh, Rinat Ofer, B. J. Ramshaw, Ruixing Liang,
D. A. Bonn, and W. N. Hardy[*]

Department of Physics and Astronomy, University of British Columbia, Vancouver, British Columbia, Canada V6T 1Z1

Huiqian Luo, Zhao-Sheng Wang, Lei Fang, and Hai-Hu Wen

*National Laboratory for Superconductivity, Institute of Physics, National Laboratory for Condensed Matter Physics,
P.O. Box 603, Beijing 100190, People's Republic of China*

We have studied the microwave electrodynamics of single-crystal iron-based superconductors $Ba_{0.72}K_{0.28}Fe_2As_2$ (hole doped, $T_c \approx 30$ K) and $Ba(Fe_{0.95}Co_{0.05})_2As_2$ (electron doped, $T_c \approx 20$ K), by cavity perturbation and broadband spectroscopy. Meissner curves were used to confirm the quality and homogeneity of the samples under study. Through cavity perturbation techniques, the temperature dependence of the in-plane London penetration depth $\Delta\lambda(T)$, and therefore the superfluid phase stiffness $\lambda^2(0)/\lambda^2(T)$ was measured. Down to 0.4 K, the data do not show the exponential saturation at low temperatures expected from a singly, fully gapped superconductor. Rather, both the electron- and the hole-doped systems seem to be best described by a power-law behavior with $\lambda^2(0)/\lambda^2(T) \sim T^n$ and $n \approx 2.5$. In the three samples we studied, a weak feature near the sensitivity limit of our measurements appears near $T/T_c = 0.04$, hinting at a corresponding low-energy feature in the superconducting density of states. The data can also be relatively well described by a simple two-gap s-wave model of the order parameter but this yields parameters which seem unrealistic and dependent on the fit range. Broadband surface resistance measurements reveal a sample-dependent residual loss whose origin is unclear. The data from the $Ba_{0.72}K_{0.28}Fe_2As_2$ samples can be made to scale as ω^2 if the extrinsic loss is treated as an additive component, indicating large scattering rates. Finally, the temperature dependence of the surface resistance at 13 GHz obeys a power law very similar to those observed for $\Delta\lambda(T)$.

I. INTRODUCTION

Tremendous interest was generated when the fluorine-doped layered compound $LaFeAsO_{1-x}F_x$ was reported to superconduct at 26 K.[1] In remarkably short time, the critical temperature of this compound was increased via pressure or chemical substitution to above 55 K, significantly higher than the highest T_c reported in any superconductor outside the cuprates [cf., MgB_2 (Ref. 2)]. Superconductivity has since been found in $Ba_{1-x}K_xFe_2As_2$ with $T_{c,max} = 38$ K,[3] and in $Ba(Fe_{1-x}Co_x)_2As_2$ with $T_{c,max} = 23$ K.[4] These so-called 122-compounds are particularly important since, unlike the cuprates or the 1111 iron pnictides, they are not oxides, eliminating the potentially problematic role of oxygen stoichiometry. Moreover, large single crystals with a variety of different cation dopings in the 122-pnictides have now been synthesized, which is essential for applying a wide range of measurements of their physical properties. The need to understand the pairing mechanism and the origin of the high T_c in any new superconductor drives a need to determine the symmetry of the order parameter. However this usually requires several different measurements to arrive at a consensus. Such measurements need to be performed on single-phase samples with well-characterized stoichiometry and sharp transitions, which imply good homogeneity; otherwise, it is challenging to compare one measurement to the next. To go even further, cation and anion disorder should also be minimized and structural information (e.g., x-ray rocking curves) should be obtained.

Historically, one powerful class of measurements that can be thought of as topological include the flux quantization measurements[5] that show superconductors are a condensate of pairs, the phase coherence measurements in bimetallic dc superconducting quantum interference devices (SQUIDs) and tunnel junctions made from single crystals of $YBa_2Cu_3O_{6+x}$ (YBCO) and thin films of the conventional s-wave superconductor Pb,[6] and the observation of half-flux quanta in geometrically frustrated junctions,[7] which were decisive in proving the extra broken symmetry in the $d_{x^2-y^2}$ state of the cuprates. Another group of measurements directly probes the superconducting pairing gap via spectroscopic means. This was famously the case in conventional s-wave superconductivity in which measurements such as tunneling,[8] infrared,[9,10] and microwave spectroscopy[11] showed a well-defined gap with a sharp threshold energy and essentially no states below the energy gap at low temperatures and in the absence of pair-breaking magnetic impurities. Such measurements were more ambiguous in the cuprates because the presence of nodes in the $d_{x^2-y^2}$ pairing state gave a characteristic energy gap scale but without the very sharp threshold and with many states available down to low energies. Angle-resolved photoemission[12,13] helped resolve this by showing the gap variation as a function of momentum around the Fermi surface.

Other measurements rely on inferring the presence of a gapped spectrum of excitations in the system by observing the temperature dependence of a wide range of features, including thermodynamic, transport, and electrodynamic properties. We will concentrate on electrodynamic characteristics here but will start with an introductory comment on the difficulties of making inferences from temperature dependen-

cies in these properties. In conventional *s*-wave superconductivity, the presence of exponentially activated behavior in many properties at low-temperature signals the presence of a nonzero minimum energy gap and hence no nodes. Such measurements[14,15] even predate BCS theory, but it has always been difficult to do this decisively since it takes high-resolution data, preferably over a few decades of the low-temperature exponential behavior, to be convincing. This has, for instance, been achieved in high-resolution measurements of the temperature-dependent microwave loss of high-*Q* resonant cavities made of Pb.[16,17]

In the case of non-*s*-wave states with nodes, the temperature dependencies tend toward various power laws. Here there is a significant challenge in identifying the particular state or even in being sure that it is not really exponentially activated. One case has proven relatively easy: the line nodes of a $d_{x^2-y^2}$ pairing state on a cylindrical Fermi surface gave rise to an unambiguous linear temperature dependence in the London penetration depth.[18] Unfortunately, disorder quickly changes this to a quadratic temperature dependence,[19] so that in materials with pair-breaking defects, especially cation doping, these techniques place high demands on resolution and careful comparison of power laws versus exponentials, plus considerable systematic work on sample dependence and multiple materials within a family. An example of this can be seen in the long effort to understand the penetration depth in the electron-doped cuprates $Pr_{2-x}Ce_xCuO_{4-\delta}$ and $Nd_{2-x}Ce_xCuO_{4-\delta}$.[20]

Universal consensus regarding the gap symmetry in the iron-based superconductors does not currently exist but the field is working hard toward remedying this situation. For example, it is known that the antiferromagnetic ground state in the $BaFe_2As_2$ parent compound is suppressed through cation substitution, thus allowing superconductivity to emerge;[4,21] being near to a magnetic state might mean that magnetic fluctuations are important for pairing and this could be reflected in the symmetry of the gap. What, then, is the pairing symmetry?

Band-structure calculations[22,23] and angle-resolved photoemission spectroscopy (ARPES) experiments[24,25] demonstrate that multiple bands cross the Fermi surface, making multiband superconductivity plausible. For the hole-doped $Ba_{1-x}K_xFe_2As_2$ compound, ARPES (Refs. 26–28) has found at least two different superconducting nodeless gaps in the *ab* plane. These results are further supported by directional point-contact Andreev-reflection spectroscopy[29] and microwave surface impedance[30] data which suggest fully, and perhaps multiply, gapped superconductivity. However, the possibility for a nodal gap has not been completely ruled out: measurements of reversible magnetization[31] and thermal Hall conductivity[32] both yield results consistent with nodes in the gap; ^{75}As nuclear magnetic resonance measurements[33] revealed the spin-lattice relaxation rate $1/T_1$ to vary close to T^3; and, muon-spin-relaxation measurements[34] exhibit a nearly linear variation in temperature of the superfluid density at low temperatures. For the electron-doped $Ba(Fe_{1-x}Co_x)_2As_2$ compound, heat transport measurements[35] suggest a nodeless superconducting gap in the *ab* plane. However, tunnel diode resonator techniques[36] have revealed that the penetration depth as a function of temperature exhibits a robust power-law (instead of exponential) behavior, with $\Delta\lambda(T) \propto T^n$ and n being between 2 and 2.5, depending on the doping level. The question of pairing symmetry remains open.

TABLE I. Transition temperatures and sample dimensions of the iron-arsenide crystals studied in this paper.

Sample	T_c (K)	*ab* surface (mm^2)	$\hat{c}$ axis (μm)	Aspect ratio
$(Ba,K)Fe_2As_2$ (A)	29.5	0.928	50	20
$(Ba,K)Fe_2As_2$ (B)	28	0.508	10	50
$Ba(Fe,Co)_2As_2$ (C)	20	1.017	5	200

II. MATERIALS AND METHODS

In this paper, we report on measurements of the temperature dependence of the London penetration depth and surface resistance in the hole-doped $Ba_{0.72}K_{0.28}Fe_2As_2$ and the electron-doped $Ba(Fe_{0.95}Co_{0.05})_2As_2$ 122-compounds. We have measured three high-quality single crystals, grown by the Wen group at the National Laboratory for Superconductivity in Beijing, using an FeAs self-flux method:[37] two of $Ba_{0.72}K_{0.28}Fe_2As_2$ and one of $Ba(Fe_{0.95}Co_{0.05})_2As_2$, with their dimensions listed in Table I. The K dopant occupies out-of-plane interstitial sites in the crystal lattice, whereas Co substitutes for Fe in the Fe_2As_2 plane. Our microwave techniques are optimized for 1 mm^2 platelets and the samples used in these measurements were carefully selected to be the best single crystals available. The sample surfaces are known to degrade from prolonged exposure to ambient atmosphere. To limit surface degradation, we have only measured samples with cleaved *ab* surfaces and between measurements, the samples were stored in a vacuum desiccator. Furthermore, these samples have little secondary impurity phase (less than 10%) as checked by specific heat.[38] Sample quality and homogeneity were confirmed via the width of the superconducting transition as a function of applied field, as shown in Fig. 1. The magnetic moment *m* of sample A, for example, was measured in dc magnetic fields applied parallel to the $\hat{c}$ axis of the crystal. In low fields (<10 G), $T_c = 30.1$ K and $\Delta T_c < 0.5$ K. At 5 T, T_c is suppressed by 15% to 25.6 K, but the transition width remains narrow ($\Delta T_c < 1.5$ K): a clear signature of a homogeneously doped sample.

A 950 MHz loop-gap resonator, described in detail elsewhere,[18] has been used to measure the temperature dependence of the surface reactance $\Delta X_S(T)$, thus allowing for a determination of $\Delta\lambda(T) = \lambda(T) - \lambda(0)$, where $\lambda(T)$ is the magnetic penetration depth. Samples are mounted on the end of a temperature-controlled sapphire plate with a small amount of silicone grease. Microwave magnetic fields are applied parallel to the *ab* plane, a geometry in which the applied magnetic field at the surface of the sample is almost everywhere equal to the applied field, and the cavity resonance frequency is measured as a function of the sample temperature. In this geometry, screening currents flow around the crystal in both the $\hat{a}$- and $\hat{c}$-axes directions. To
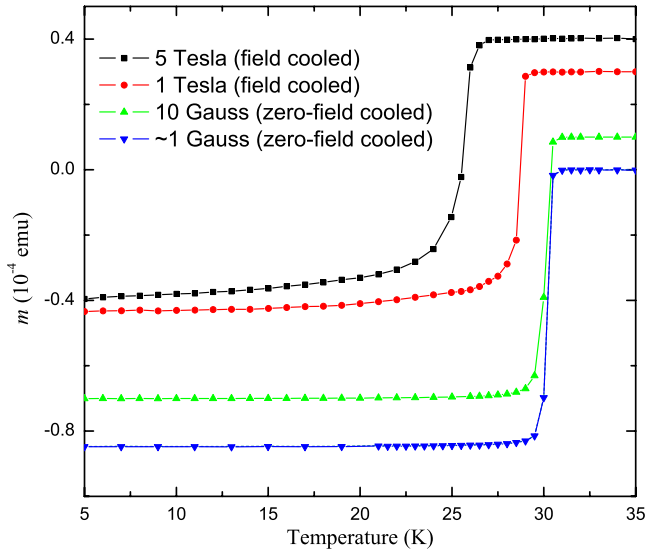
FIG. 1. (Color online) The magnetic moment m of the $Ba_{0.72}K_{0.28}Fe_2As_2$ sample A, as measured by a (Quantum Design Magnetic Property Measurement System) SQUID magnetometer. The data have been multiplicatively scaled to fit on the same plot. Even at high applied magnetic fields, the width of the superconducting transition remains sharp.

limit the effects of $\hat{c}$-axis contamination, platelets with large a/c aspect ratios are preferred. When the system is run as an oscillator (rather than as a conventional resonator), an absolute frequency stability of ~ 0.1 Hz/min provides subangstrom resolution in $\Delta\lambda(T)$ measurements. The samples were cooled to 1.2 K via a ^{4}He pumped cryostat, and to 0.4 K via a ^{3}He pot and a charcoal sorption pump at 4.2 K. The resonator remained at 1.2 K, in direct contact with a pumped ^{4}He bath, throughout the experiment.

Surface resistance $R_S(\omega, T)$ measurements were made using a recently developed nonresonant broadband microwave apparatus operating between 0.5 and 20 GHz, described in detail elsewhere.[39] As with the above technique, microwave magnetic fields are applied parallel to the ab plane. The microwave power is modulated at low frequency and the measured temperature oscillation of the superconducting sample gives a direct measure of the absorbed power. A reference alloy of Ag:Au, placed in an electromagnetically equivalent position as the superconducting sample, is then used to calibrate the absolute surface resistance of the FeAs crystal. The temperature dependence of $\Delta R_S(T)$ was measured at 13 GHz in the axial microwave magnetic fields of the TE_{011} modes of a right-circular cylindrical cavity, described elsewhere.[40]

III. PENETRATION DEPTH RESULTS

The measured magnetic penetration depth for all three samples is shown in Fig. 2 as a function of temperature. The measured background frequency shift from an empty sapphire plate with a small amount of silicone grease (approximately equal to that used to hold the sample in place) corresponds to about 0.2 Å in $\Delta\lambda$ at base temperature and shows no systematic temperature dependence. The penetration
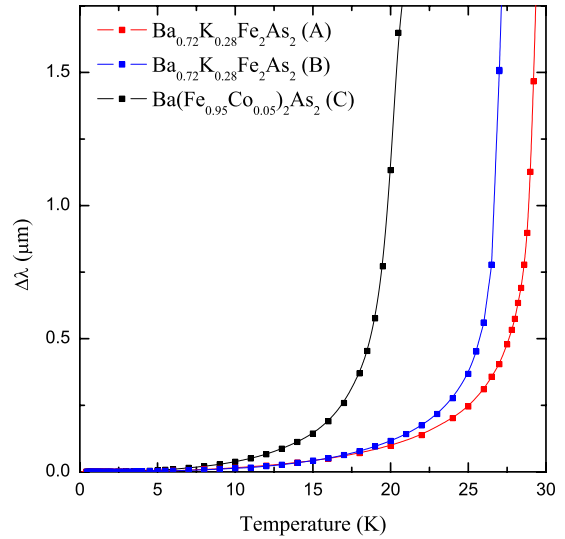

FIG. 2. (Color online) The change in the London penetration depth, $\lambda(T) - \lambda(0)$, as a function of temperature for all three samples. Solid lines are a guide to the eyes.

depth of both K-doped crystals (samples A and B) has also been measured in a 12 kHz ac susceptometer, described in detail elsewhere[41] and, to within calibration uncertainties, agrees with the 950 MHz cavity perturbation measurements.

Before fitting models to the data, an anomaly that appears near $T/T_c \approx 0.04$ in the measured $\Delta\lambda$ of all three samples is shown in Fig. 3. That the anomaly scales with T_c is likely an indication that the feature is relevant and may be related to the onset of magnetic order in the crystals; for example, samples A and B are in the doping range where coexistence of a spin-density wave and superconductivity has been reported,[42] and sample C has a doping level which is very close to where antiferromagnetism has been observed to coexist with superconductivity.[4,43] Concern that this feature
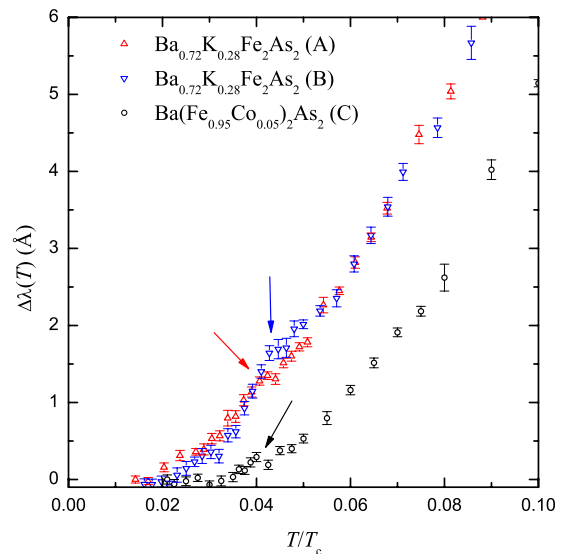

FIG. 3. (Color online) The anomalous "bump" in the London penetration depth. For all three samples, the bump occurs at $T/T_c \approx 0.04$.
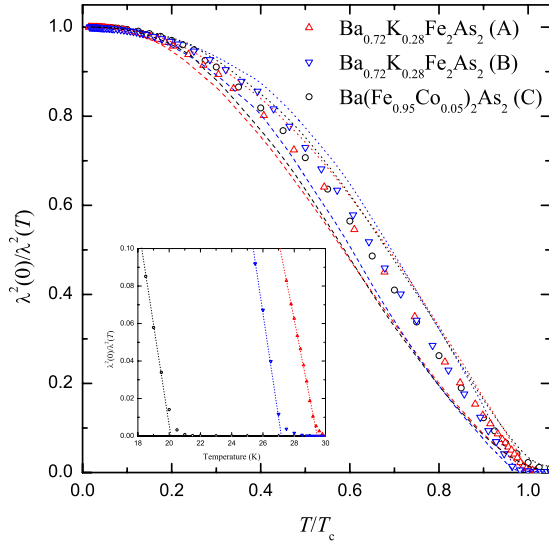
FIG. 4. (Color online) Extracted superfluid density of all three samples, using three different choices of $\lambda(0)$ (symbols are 2000 Å, dashed lines are 1500 Å, and dotted lines are 2500 Å). Inset: the superfluid transition of all three samples. Dotted lines are linear guide to the eyes and show that deviations from linearity occur only very near T_c in the form of feet that indicate minor inhomogeneities in the T_c of the sample.

might be due to a trace contaminant, such as a small particle of superconducting aluminum metal, led us to remeasure after carefully recleaning the samples and sapphire. The anomaly persisted and its origin in the bulk properties of the sample remains uncertain. Due to its small magnitude, one can seek to model the overall low-temperature behavior without explicitly addressing its presence.

The temperature dependence of the penetration depth provides access to the superfluid density or, more correctly, the superfluid phase stiffness, provided one has a measure of $\lambda(T_0)$, where T_0 is some suitably low temperature. Figure 4 shows the extracted superfluid phase stiffness for all three samples. For the analysis that follows, we take $\lambda(0)$ =2000 Å,[44] but Fig. 4 shows that the choice of $\lambda(0) \pm 25\%$ does not affect the qualitative features of the superfluid density.

At higher temperatures, the superfluid phase stiffness approaches T_c approximately linearly, as shown in the inset of Fig. 4, consistent with mean-field behavior. Small deviations from linearity occur about 0.5 K from T_c. The onset of curvature is likely a result of small sample inhomogeneity. There appears to be no evidence for the three-dimensional XY critical fluctuation behavior seen in very high-quality YBa$_2$Cu$_3$O$_{7-\delta}$ samples[45] where $\lambda^2(0)/\lambda^2(T)$ approaches T_c with infinite, rather than finite, slope. The present iron arsenide crystals under study appear quite homogeneous, especially when compared to the broad "feet" seen in the superfluid density near T_c in some measurements.[30,46,47]

The temperature dependence upon approaching $T=0$ provides the strongest constraints on possible nodes in the superconducting gap since low temperatures query the lowest energy excitations in the system. At the lowest temperatures, there exist a number of different models, each of which are

motivated by physically realizable scenarios. The simple s-wave BCS model[48] that, at low temperatures, takes the form

$$\frac{\lambda(T)}{\lambda(0)} \approx \sqrt{\frac{2\pi\Delta_0}{k_B T}} \exp\left(\frac{-\Delta_0}{k_B T}\right), \tag{1}$$

does not fit the data well at all, and additionally yields uncharacteristically small gaps of $2\Delta/k_B T_c \approx 1.5$ under the best-fit conditions for the K-doped samples A and B, and $2\Delta/k_B T_c \approx 2.0$ under the best-fit conditions for the Co-doped sample C. The best-fit curves are not shown.

Also worth considering is whether the deviation $\Delta\lambda(T)$ is quadratic in temperature. A T^2 temperature dependence of the penetration depth for $T \ll T_c$ is expected for a superconducting gap with line nodes; e.g., d-wave symmetry, in the presence of strong scattering, which will create an additional quasiparticle density of states.[19] This deviation from otherwise linear behavior of $\Delta\lambda(T)$ predicted for a d-wave gap symmetry is expected to occur only below a characteristic temperature $T^\star$, controlled by the impurity concentration. The T^2 model we apply to the superfluid phase stiffness takes the form

$$\frac{\lambda^2(0)}{\lambda^2(T)} \approx 1 - \left(\frac{T}{T^\star}\right)^2. \tag{2}$$

The quadratic temperature dependence fits to the data work moderately well (not shown) and return values of $T^\star \approx T_c$, which is not surprising, as so much scattering should suppress T_c. It is worth noting that T^2 variation in the superfluid density at the lowest temperatures has been observed before, in YBCO films[49] and crystals[50] of relative poor quality. Also worth noting is that within the $s_\pm$-wave model with impurity scattering,[51] some low-energy quasiparticle excitations can occur leading to a power-law like dependence, such as a density of states proportional to E^2.

The data can be reasonably well described by a two-gap s-wave model,[52] which might be an appropriate starting point for a superconductor with multiple Fermi-surface sheets. At very low temperatures, the change in superfluid phase stiffness with temperature is dominated by the smallest gap, with the larger gap becoming more apparent at high temperatures. The main role of the large gap in modeling the low-temperature data is to limit the rapid rise in penetration depth if a small gap were allowed to dominate a large fraction of the Fermi surface in the Brillouin zone. The model applied takes the form

$$\frac{\lambda^2(0)}{\lambda^2(T)} \approx 1 - x\sqrt{\frac{2\pi\Delta_{0,S}}{k_B T}} \exp\left(\frac{-\Delta_{0,S}}{k_B T}\right)$$
$$- (1-x)\sqrt{\frac{2\pi\Delta_{0,L}}{k_B T}} \exp\left(\frac{-\Delta_{0,L}}{k_B T}\right), \tag{3}$$

where $x = \lambda^2(0)/\lambda_S^2(0)$ and is the fractional contribution of the small gap $\Delta_{0,S}$ to the total superfluid density. These fits are shown as the solid black lines in Fig. 5. The gap sizes obtained from the two-gap model are small: $\Delta_{0,S}$ is nearly five times smaller than $\Delta_{0,L}$, and both are less than the weak-coupling BCS expectation of $2\Delta/k_B T_c \approx 3.5$.
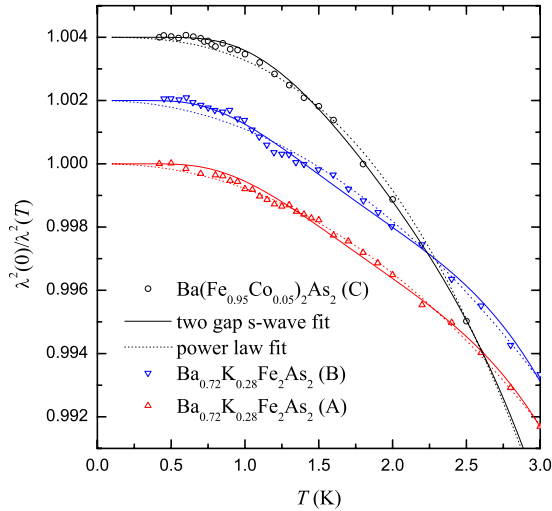
FIG. 5. (Color online) Two gap s-wave [solid line, Eq. (3)] and power-law [dashed line, Eq. (4)] fits over 0–3 K to the superfluid phase stiffness. Notice the very fine scale of $\lambda^2(0)/\lambda^2(T)$. For clarity, the superfluid phase stiffness of samples C and B have been shifted vertically by 0.004 and 0.002, respectively.

Finally, we attempt fits to a power law,

$$\frac{\lambda^2(0)}{\lambda^2(T)} \approx 1 - \left(\frac{T}{T^\star} \right)^n. \qquad (4)$$

In clean superconductors, the deviation $\Delta\lambda$ of the penetration depth from its zero-temperature value $\lambda(0)$ is proportional to T^n and unveils the topology of the superconducting gap. Specifically, $n=1$ for line nodes and $n=2$ for point nodes. Nonlocal effects, impurities, and other defects serve to increase the exponent n;[19] consequently, deciphering the curious exponent n relies upon whether it is larger or smaller than 2. The dashed lines of Fig. 5 show how a power law with $n \approx 2.5$ can be used to describe the superfluid density of these samples at low temperatures. This power law is in agreement with previous penetration depth measurements.[36]

For samples A and B, the data is best described by a power law (as determined by a χ^2 statistic), regardless of the temperature range over which the fit is applied. For sample C, both a power-law fit and a two-gap fit describe the data equally well. Table II shows the extracted fit parameters for each model. Note that the fit parameters systematically increase as the fit range is increased for the two-gap model while there is no such systematic deviation in the parameters for the power-law fits. As the 122-system is studied over successively smaller temperature ranges, it appears as though the parameters extracted from two-gap models always seem to tend toward a very small gap on an insignificant fraction of the Fermi surface.

IV. MICROWAVE SPECTROSCOPY RESULTS

Well below T_c, most superconducting properties should depend strongly on the quasiparticle excitations near the nodes (or minima) of the gap function. Important signatures of nodal-quasiparticle transport emerge in the frequency de-

pendence of the in-plane microwave conductivity, $\sigma_1(\omega,T)$, which is extracted from measurements of $R_S(\omega,T)$. Specifically, at low temperature, the surface resistance is related to the conductivity via the relation[53]

$$R_S(\omega,T) \simeq \frac{1}{2}\mu_0^2\omega^2\lambda^3(T)\sigma_1(\omega,T). \qquad (5)$$

$R_S(\omega,T)$ spectra of the two $Ba_{0.72}K_{0.28}Fe_2As_2$ samples B and A are shown in Figs. 6 and 7, respectively. There is a significant difference in the low-temperature surface resistance between the two samples. At 20 GHz and 3 K, the R_S of the thick sample A is roughly 3.5 times larger than that of the thin sample B. The same is not true, however, at higher temperatures. At 20 GHz and 15 K, the R_S of the two samples are now much closer and differ only by 30%. This could be the result of an extrinsic temperature-independent residual loss (of unknown origin), dominant when the sample itself shows little loss and obscured when the sample loss is sufficiently high.

Another indication that the low-temperature loss might be extrinsic is that at $T=15$ K in the lower loss sample, shown in Fig. 6, R_S is proportional to ω^2, a result expected if there is sufficient scattering to yield conductivity $\sigma_1(\omega)$ that is independent of frequency in the microwave range. Elimination of the residual component is performed by subtracting the loss at the lowest measured temperature, a procedure which has been shown to work for s-wave superconductors.[16] Doing this reveals that the absolute temperature evolution of $R_S(\omega,T)$ is the same for both samples, as highlighted by the plot of $\Delta R_S(\omega,T)=R_S(\omega,T)-R_S(\omega,T_0)$ in Fig. 8, supporting the hypothesis of an extrinsic residual loss. Specifically, Fig. 8 demonstrates that the resulting loss after subtraction seems to be intrinsic, in that it has the same temperature and ω^2 dependence in both samples. Making this subtraction, however, removes the possibility of being able to state whether or not some intrinsic residual resistivity actually does exist.

In the $Ba_{0.72}K_{0.28}Fe_2As_2$ samples A and B, it is very likely that the K dopants are the dominant source of quasiparticle scattering. With such a high concentration (28%) of dopants, it is reasonable to expect that the widths of the quasiparticle conductivity spectra lie well outside of our measurement bandwidth. In this case, the in-plane microwave conductivity $\sigma_1(\omega,T) \approx 2R_S(\omega,T)/\mu_0^2\omega^2\lambda^3(T)$ would appear frequency independent, resulting in the $R_S(\omega,T) \sim \omega^2$ as shown by the lines in Fig. 8.

There exist a number of factors that might account for the observed excess loss in the $Ba_{0.72}K_{0.28}Fe_2As_2$ samples and surface contamination (perhaps a barium oxide layer) seems to be the most likely source. Both samples A and B were cleaved from a larger crystal before they were measured with one potentially significant difference: while one surface of sample A was cleaved just prior to the start of measurements, the opposite surface had been cleaved weeks earlier allowing for the possibility of enhanced degradation of that surface. Sample B, on the other hand, had both surfaces freshly cleaved immediately before measurements began.

A second possible source of the observed excess loss is the presence of delaminated edges on the samples. Sample

TABLE II. Parameters from two-gap *s*-wave and power-law fits. For sample A, the data is best described by the power law T^n with $n \approx 2.26 \pm 0.08$. For sample B, the data is best described by the power law T^n with $n \approx 2.10 \pm 0.02$. For sample C, both a two-gap *s*-wave model and a power-law model T^n with $n \approx 2.66 \pm 0.09$ describe the data equally well over all temperature ranges.

Sample A	Two gap			Power law	
Fit range T_{max} (K)	x (%)	$\frac{2\Delta_{0,S}}{k_B T_c}$	$\frac{2\Delta_{0,L}}{k_B T_c}$	n	$T^\star$ (K)
3	0.9	0.30	1.65	2.15	28.0
4	1.2	0.34	1.84	2.22	25.8
5	1.8	0.41	2.08	2.25	24.9
6	2.5	0.48	2.26	2.31	23.8
7	3.3	0.54	2.40	2.35	23.0

Sample B	Two gap			Power law	
Fit range T_{max} (K)	x (%)	$\frac{2\Delta_{0,S}}{k_B T_c}$	$\frac{2\Delta_{0,L}}{k_B T_c}$	n	$T^\star$ (K)
3	0.8	0.29	1.69	2.07	29.3
4	1.2	0.34	1.94	2.11	27.9
5	1.8	0.42	2.24	2.11	28.1
6	2.6	0.50	2.49	2.09	28.5
7	3.3	0.56	2.67	2.11	27.9

Sample C	Two gap			Power law	
Fit range T_{max} (K)	x (%)	$\frac{2\Delta_{0,S}}{k_B T_c}$	$\frac{2\Delta_{0,L}}{k_B T_c}$	n	$T^\star$ (K)
3	2.1	0.57	2.24	2.73	14.1
4	3.6	0.70	2.62	2.60	15.4
5	4.0	0.72	2.75	2.53	16.2
6	3.5	0.69	2.66	2.75	14.4
7	4.1	0.74	2.71	2.70	14.7

edges that resemble the unbound leafy edge of a book present obvious problems for microwave measurements. In the extreme case, the microwave fields would be allowed to penetrate the regions between loosely connected "sheets" of the sample. Currents that loop around the sample are presented with a tortuous path near the edges that increases the effective surface area of the sample. In fact, preliminary measurements of $\Delta\lambda(T)$ by our group on early samples with obvious edge problems showed a linear temperature dependence that had an unrealistic slope of ~ 200 Å/K, cf. YBCO that has $\Delta\lambda(T) \approx 4$ Å/K.[45] Scanning electron microscope images, as in Fig. 9, have confirmed that some crystals do show signs of delaminated edges with sheets $\approx 1-2$ μm thick. This effect is therefore suppressed for the thinner $Ba_{0.72}K_{0.28}Fe_2As_2$ sample B [and the $Ba(Fe_{0.95}Co_{0.05})_2As_2$ sample C], compared to the thicker sample A, measured in this work. This effect touches upon a slightly different issue than the surface degradation problem mentioned above, since it could affect the data in a multiplicative way, not just additively; however, it is an effect worth noting as yet another reason to work on only very thin and freshly cleaved samples.

It also seems possible that intrinsic $\hat{c}$-axis contamination was providing the excess loss. However, the thicker sample A was cut into two pieces such that any $\hat{c}$-axis contribution to the $R_S(T)$ measurements would be enhanced (doubled) but such enhancement was not observed in the measurements.

Despite falling well outside the measurement bandwidth, it is possible to obtain an estimate of the spectral width Γ through the oscillator-strength sum rule. [Our broadband system measures $\sigma_1(\omega, T)$ out to $\omega/2\pi = 20$ GHz and in this spectral region we find $\sigma_1(\omega, T)$ is independent of ω and therefore no direct measure of the width of the conductivity spectrum can be obtained.] The oscillator-strength sum rule is given by

$$\frac{n_n(T)e^2}{m^*} = \frac{2}{\pi} \int_0^\infty \sigma_1(\omega, T) d\omega. \qquad (6)$$

As the temperature is raised, any spectral weight depleted from the superfluid density $n_s(T)$ must reappear as an increase in the frequency-integrated quasiparticle conductivity. One can approximate the integral on the right-hand side of
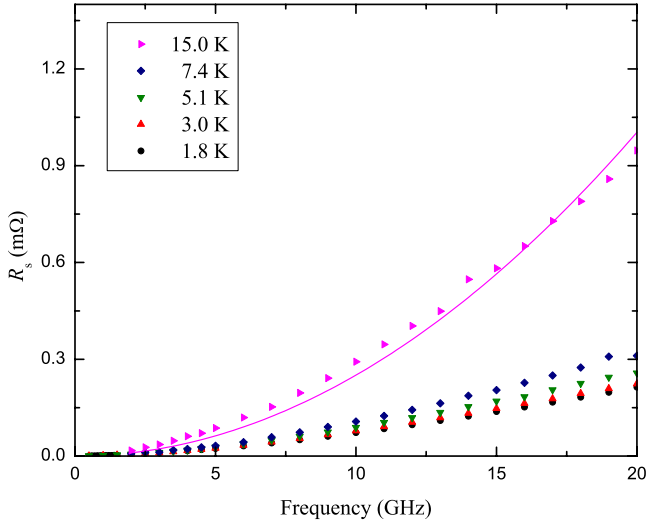
FIG. 6. (Color online) In-plane surface resistance of sample B from 0.5 to 20 GHz. The loss of the sample B at 20 GHz and base temperature is a factor of 3.5 less than that of sample A. The solid line is $\propto \omega^2$.

Eq. (6) to be equal to $\sigma_0 \Gamma$, and the left-hand side of Eq. (6) is determined by partitioning the conduction electron density n into a superfluid density n_s and a normal-fluid density $n_n = n - n_s \sim 1/\lambda^2(0) - 1/\lambda^2(T)$, corresponding to quasiparticles thermally excited from the condensate. In so doing, we make use of $\sigma_0 \approx 2R_S(\omega,T)/\mu_0^2 \omega^2 \lambda^3(T)$ being the extrapolated value of $\sigma_1(\omega \to 0)$ and Γ as a measure of the spectral width of $\sigma_1(\omega,T)$. From this generalized two-fluid model,[54] the value of n_s (and its temperature dependence) is determined from measurements of the magnetic penetration depth and recalling the definition of the London penetration depth $\lambda_L^{-2} = \mu_0 n_s e^2/m^*$. The temperature dependence of the spectral widths of samples A and B so determined are shown in Fig. 10. These values of $\Gamma/2\pi$ are more than an order of magnitude larger then what has been observed in YBCO (Ref. [55]) and show no clear temperature dependence; their magni-
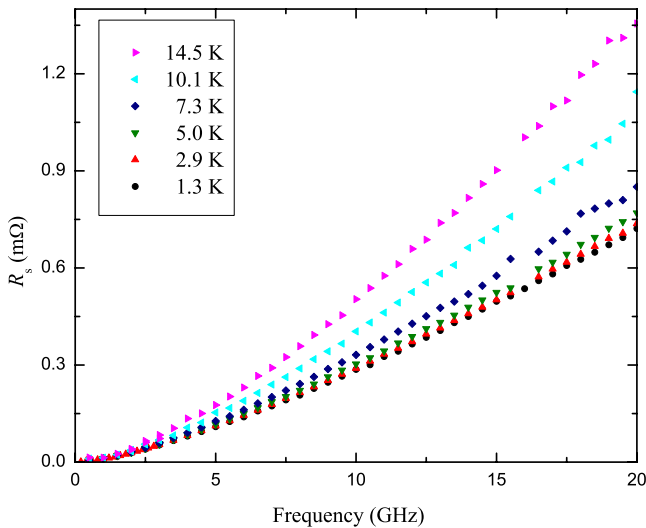
tudes, however, are comparable to the low-temperature scattering rates of $Bi_2Sr_2CaCu_2O_{8+\delta}$ derived from terahertz spectroscopy.[56]

Finally, Fig. 11 shows the temperature dependence of $\Delta R_S(\omega,T)$ at 13 GHz for a variety of superconductors. For each of the conventional BCS s-wave superconductors ($Pb_{0.95}Sn_{0.05}$, Nb, and Sn), $\Delta R_S(\omega,T)$ scales as T/T_c and shows a very weak temperature dependence below $T/T_c = 0.4$. The $Ba_{0.72}K_{0.28}Fe_2As_2$ data, on the other hand, shows no signs of flattening and obeys a power law $R_S(\omega,T) \propto T^n$ down to the lowest measurement temperature. Fits up to $T/T_c = 0.5$ give $n \approx 2.5 \pm 0.3$, which is the temperature dependence expected for a normal fluid density that tracks the loss of superfluid density. Rigorous comparisons to the low-T power-law fits to the superfluid phase stiffness, however, are not possible because the $\Delta R_S(\omega,T)$ do not extend to low
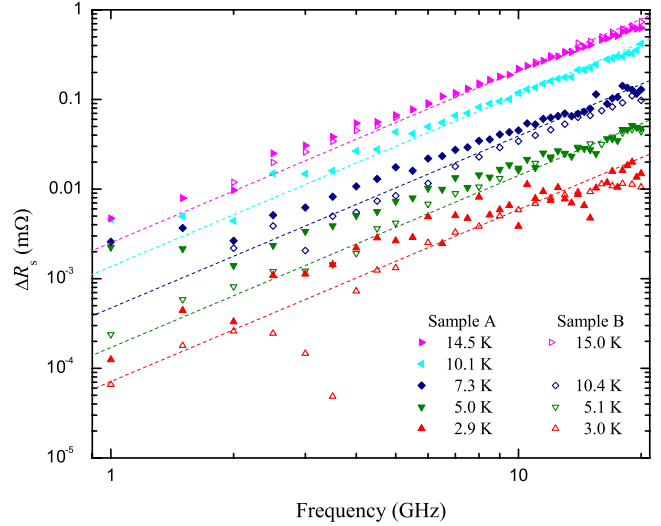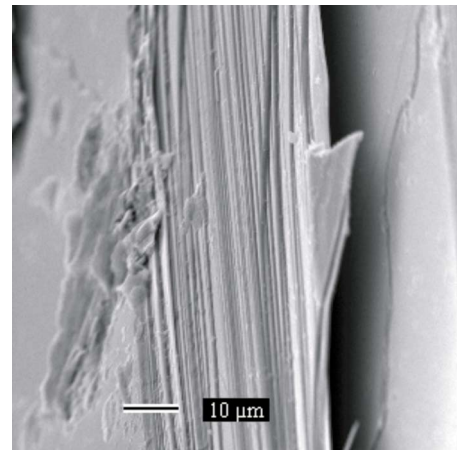

FIG. 8. (Color online) $\Delta R_S(\omega,T) = R_S(\omega,T) - R_S(\omega,T_0)$ for samples A (solid symbols) and B (open symbols). $\Delta R_S(\omega,T)$ is seen to be the same for both samples indicating that sample A (the thicker of the two) has an extra temperature-independent loss. The dashed lines have a slope of 2 ($\Delta R_S \propto \omega^2$).

FIG. 7. (Color online) In-plane surface resistance of sample A from 0.5 to 20 GHz.

FIG. 9. (Color online) Scanning electron microscope image of the edge of a platelet $Ba_{0.72}K_{0.28}Fe_2As_2$ crystal, showing delaminated edges.
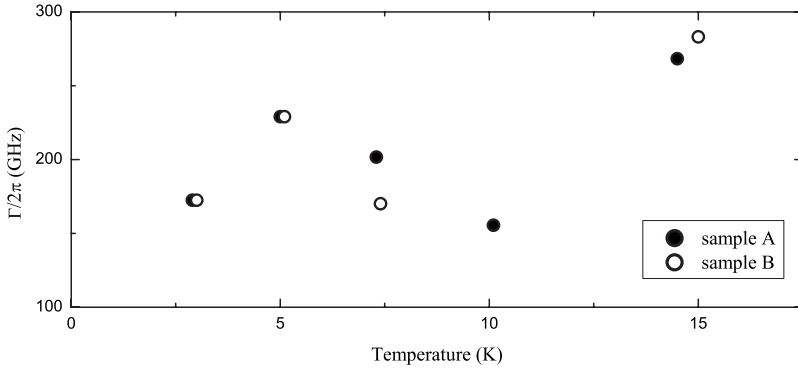
FIG. 10. Estimates of the quasiparticle conductivity spectral widths $\Gamma/2\pi$ of samples A and B as a function of temperature.

enough base temperatures and the resolution of the measurement at the lowest temperatures is inadequate. Nevertheless, it is clear that the overall temperature dependence of the surface resistance of the $Ba_{0.72}K_{0.28}Fe_2As_2$ samples differs significantly from that of the *s*-wave BCS superconductors.

The surface resistance of ortho-II ordered $YBa_2Cu_3O_{6.52}$ (gray open symbols of Fig. 11) shows a low-temperature peak (as does the quasiparticle conductivity). This peak results from a competition between the temperature dependencies of the normal fluid density and of the quasiparticle scattering rates; at lower temperatures it is the reduced normal fluid density which wins out over large scattering rates, while the converse is the case at higher temperatures.[40,57] This feature is known to be extremely sensitive to disorder and/or impurities,[58] and considering that the spectral width of the quasiparticle conductivity of $Ba_{0.72}K_{0.28}Fe_2As_2$ is estimated to be an order of magnitude larger than it is in ortho-II ordered $YBa_2Cu_3O_{6.52}$, the absence of a peak in $R_S(\omega, T)$ is not surprising, even though there may be a modest decrease in the scattering rate below T_c.

Because the broadband measurements have revealed an excess extrinsic loss in our $Ba_{0.72}K_{0.28}Fe_2As_2$ samples, it is not possible to obtain reliable quasiparticle conductivities from our $R_S(T)$ measurements. The exact behavior of $\sigma_1(T)$ necessitates simultaneous measurements of $R_S(T)$ and $X_S(T)$. Limited to what we can extract, an approximated quasiparticle conductivity, we see no evidence of a coherence peak just below T_c. This is in contrast to what has been previously reported,[30] but those conclusions were drawn from a broad, nearly 5 K wide enhancement in the quasiparticle conductivity just below T_c in a sample whose superconducting transition temperature width $\Delta T_c \approx 2.5$ K. The behavior of $\sigma_1(T)$ is known to be highly susceptible to inhomogeneity broadening of the superconducting transition. Similar quasiparticle conductivity enhancements below T_c were observed early on in the cuprates[50,59] but were later attributed to broadened superconducting transitions.[60–62] The samples studies in this paper have $\Delta T_c \approx 0.5$ K and we extract a much narrower, sharp cusp (only 0.5 K wide, not shown in this paper) that can be attributed to superconducting critical fluctuations, rather than evidence of a coherence peak. We do, however, observe the same lower peak associated with the quasiparticle scattering rate (also not shown in this paper).

V. CONCLUSIONS

We have measured the microwave electrodynamics of single-crystal iron-based superconductors $Ba_{0.72}K_{0.28}Fe_2As_2$

(hole doped, $T_c \approx 30$ K) and $Ba(Fe_{0.95}Co_{0.05})_2As_2$ (electron doped, $T_c \approx 20$ K), by cavity perturbation and broadband spectroscopy.

Sample quality and homogeneity were confirmed with a SQUID magnetometer via the width of the superconducting transition as a function of applied field. Penetration depth measurements further confirm that these samples were homogeneously doped, especially when compared with the sharpness of the transitions in other published superfluid measurements, which show a wide range of feet above T_c.

Using a 950 MHz loop-gap resonator (with results checked against a 12 kHz ac susceptometer), we were able to measure $\Delta\lambda(T)$ with subangstrom resolution down to 0.4 K. An anomaly in $\Delta\lambda$, common to all three samples, occurred at $T/T_c \approx 0.04$. While the source of this feature is not currently understood, we have ruled out contaminants on the sample surface and systematic background signals associated with the experimental apparatus. Four separate mathematical models were fit to the superfluid phase stiffness, extracted from the $\Delta\lambda(T)$ data, over a temperature range, which extends up to 20% of T_c. For the $Ba_{0.72}K_{0.28}Fe_2As_2$ samples, the behavior is best described by a power law with $T^{2.5}$. The
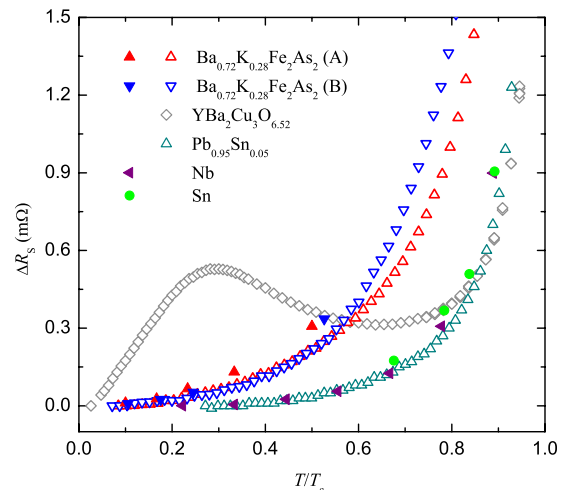

FIG. 11. (Color online) $\Delta R_S(\omega, T)$ at 13 GHz as a function of T/T_c for several superconductors. Solid symbols were taken using the broadband spectrometer. Open symbols were taken using a 13 GHz resonator. The conventional *s*-wave superconductors ($Pb_{0.95}Sn_{0.05}$, Nb, and Sn) exhibit a very weak temperature dependence for $T/T_c < 0.4$. The $Ba_{0.72}K_{0.28}Fe_2As_2$ samples obey a power law $\Delta R_S(\omega, T) \propto T^\gamma$ down to the lowest measurement temperature.

data was also relatively well described with a two-gap *s*-wave model, although the fit parameters (x, $\Delta_{0,S}$, and $\Delta_{0,L}$) all systematically increase as the fit range is increased. Moreover, x is very small resulting in unbalanced contributions to $1/\lambda^2(0)$ from the small and large gaps, and the gap values are always smaller than the BCS weak-coupling result: $2\Delta_{0,L,S}/k_B T_c < 3.5$. These are perhaps all indications that the *s*-wave two-gap scenario is not the correct picture for the 122-pnictides. Alternatively, if interband coupling is strong, a multiple gap scenario could persist, however it may not then be appropriate to treat the gaps independently. For the Ba(Fe$_{0.95}$Co$_{0.05}$)$_2$As$_2$ sample, both the power law and the two-gap *s*-wave models seemed to work equally well. None of the data is very well described with a T^2 fit.

We have also taken broadband surface resistance measurements, from 1–20 GHz, which reveal a sample-dependent residual loss in the Ba$_{0.72}$K$_{0.28}$Fe$_2$As$_2$ samples whose origin is unclear. An additive extrinsic loss is posited, from which an underlying intrinsic behavior common to both samples can be recovered by subtracting the lowest tempera-ture measure of $R_S(\omega)$. In so doing, both Ba$_{0.72}$K$_{0.28}$Fe$_2$As$_2$ samples follow a nearly ω^2 trend. The direct implication is that the quasiparticle conductivity is frequency independent up to our highest frequency of 20 GHz. This is consistent with our estimates of the quasiparticle scattering rates which are in the range of 150–270 GHz, much higher than those seen in YBCO but comparable to the rates observed in BSSCO.

ACKNOWLEDGMENTS

*hardy@phas.ubc.ca

[1] Y. Kamihara, T. Watanabe, M. Hirano, and H. Hosono, J. Am. Chem. Soc. **130**, 3296 (2008).

[2] J. Nagamatsu, N. Nakagawa, T. Muranaka, Y. Zenitani, and J. Akimitsu, Nature (London) **410**, 63 (2001).

[3] M. Rotter, M. Tegel, D. Johrendt, I. Schellenberg, W. Hermes, and R. Pöttgen, Phys. Rev. B **78**, 020503 (2008).

[4] N. Ni, M. E. Tillman, J.-Q. Yan, A. Kracher, S. T. Hannahs, S. L. Bud'ko, and P. C. Canfield, Phys. Rev. B **78**, 214515 (2008).

[5] C. E. Gough, M. S. Colclough, E. M. Forgan, R. G. Jordan, M. Keene, C. M. Muirhead, A. I. M. Rae, N. Thomas, J. S. Abell, and S. Sutton, Nature (London) **326**, 855 (1987).

[6] D. A. Wollman, D. J. Van Harlingen, W. C. Lee, D. M. Ginsberg, and A. J. Leggett, Phys. Rev. Lett. **71**, 2134 (1993).

[7] C. C. Tsuei, J. R. Kirtley, C. C. Chi, L. S. Yu-Jahnes, A. Gupta, T. Shaw, J. Z. Sun, and M. B. Ketchen, Phys. Rev. Lett. **73**, 593 (1994).

[8] I. Giaever, Phys. Rev. Lett. **5**, 147 (1960).

[9] D. M. Ginsberg and M. Tinkham, Phys. Rev. **118**, 990 (1960).

[10] P. L. Richards and M. Tinkham, Phys. Rev. **119**, 575 (1960).

[11] J. P. Turneaure and I. Weissman, J. Appl. Phys. **39**, 4417 (1968).

[12] Z.-X. Shen, D. S. Dessau, B. O. Wells, D. M. King, W. E. Spicer, A. J. Arko, D. Marshall, L. W. Lombardo, A. Kapitulnik, P. Dickinson, S. Doniach, J. DiCarlo, A. G. Loeser, and C. H. Park, Phys. Rev. Lett. **70**, 1553 (1993).

[13] H. Ding, M. R. Norman, J. C. Campuzano, M. Randeria, A. F. Bellman, T. Yokoya, T. Takahashi, T. Mochiku, and K. Kadowaki, Phys. Rev. B **54**, R9678 (1996).

[14] W. S. Corak, B. B. Goodman, C. B. Satterthwaite, and A. Wexler, Phys. Rev. **102**, 656 (1956).

[15] W. S. Corak and C. B. Satterthwaite, Phys. Rev. **102**, 662 (1956).

[16] J. P. Turneaure, Ph.D. thesis, Stanford University, 1967.

[17] J. Halbritter, Z. Phys. **238**, 466 (1970).

[18] W. N. Hardy, D. A. Bonn, D. C. Morgan, R. Liang, and K. Zhang, Phys. Rev. Lett. **70**, 3999 (1993).

[19] P. J. Hirschfeld and N. D. Goldenfeld, Phys. Rev. B **48**, 4219 (1993).

[20] J. D. Kokales, P. Fournier, L. V. Mercaldo, V. V. Talanov, R. L. Greene, and S. M. Anlage, Phys. Rev. Lett. **85**, 3696 (2000).

[21] M. Rotter, M. Tegel, and D. Johrendt, Phys. Rev. Lett. **101**, 107006 (2008).

[22] V. Barzykin and L. P. Gorko'kov, JETP Lett. **88**, 131 (2008).

[23] V. Cvetkovic and Z. Tesanovic, EPL **85**, 37002 (2009).

[24] C. Liu, G. D. Samolyuk, Y. Lee, N. Ni, T. Kondo, A. F. Santander-Syro, S. L. Bud'ko, J. L. McChesney, E. Rotenberg, T. Valla, A. V. Fedorov, P. C. Canfield, B. N. Harmon, and A. Kaminski, Phys. Rev. Lett. **101**, 177005 (2008).

[25] D. V. Evtushinsky, D. S. Inosov, V. B. Zabolotnyy, A. Koitzsch, M. Knupfer, B. Buchner, M. S. Viazovska, G. L. Sun, V. Hinkov, A. V. Boris, C. T. Lin, B. Keimer, A. Varykhalov, A. A. Kordyuk, and S. V. Borisenko, Phys. Rev. B **79**, 054517 (2009).

[26] H. Ding, P. Richard, K. Nakayama, K. Sugawara, T. Arakane, Y. Sekiba, A. Takayama, S. Souma, T. Sato, T. Takahashi, Z. Wang, X. Dai, Z. Fang, G. F. Chen, J. L. Luo, and N. L. Wang, EPL **83**, 47001 (2008).

[27] L. Zhao, H.-Y. Liu, W.-T. Zhang, J.-Q. Meng, X.-W. Jia, G.-D. Liu, X.-L. Dong, G.-F. Chen, J.-L. Luo, N.-L. Wang, W. Lu, G.-L. Wang, Y. Zhou, Y. Zhu, X.-Y. Wang, Z.-Y. Xu, C.-T. Chen, and X.-J. Zhou, Chin. Phys. Lett. **25**, 4402 (2008).

[28] K. Nakayama, T. Sato, P. Richard, Y.-M. Xu, Y. Sekiba, S. Souma, G. F. Chen, J. L. Luo, N. L. Wang, H. Ding, and T. Takahashi, EPL **85**, 67002 (2009).

[29] P. Szabó, Z. Pribulová, G. Pristáš, S. L. Bud'ko, P. C. Canfield, and P. Samuely, Phys. Rev. B **79**, 012503 (2009).

[30] K. Hashimoto, T. Shibauchi, S. Kasahara, K. Ikada, S. Tonegawa, T. Kato, R. Okazaki, C. J. van der Beek, M. Konczykowski, H. Takeya, K. Hirata, T. Terashima, and Y. Matsuda, Phys. Rev. Lett. **102**, 207001 (2009).

[31] S. Salem-Sugui, Jr., L. Ghivelder, A. D. Alvarenga, J. L. Pimen-

tel, Jr., H. Luo, Z. Wang, and H.-H. Wen, Phys. Rev. B **80**, 014518 (2009).

[32] J. G. Checkelsky, L. Li, G. F. Chen, J. L. Luo, N. L. Wang, and N. P. Ong, arXiv:0811.4668 (unpublished).

[33] H. Fukazawa, T. Yamazaki, K. Kondo, Y. Kohori, N. Takeshita, P. M. Shirage, K. Kihou, K. Miyazawa, H. Kito, H. Eisaki, and A. Iyo, J. Phys. Soc. Jpn. **78**, 033704 (2009).

[34] T. Goko, A. A. Aczel, E. Baggio-Saitovitch, S. L. Bud'ko, P. C. Canfield, J. P. Carlo, G. F. Chen, P. Dai, A. C. Hamann, W. Z. Hu, H. Kageyama, G. M. Luke, J. L. Luo, B. Nachumi, N. Ni, D. Reznik, D. R. Sanchez-Candela, A. T. Savici, K. J. Sikes, N. L. Wang, C. R. Wiebe, T. J. Williams, T. Yamamoto, W. Yu, and Y. J. Uemura, Phys. Rev. B **80**, 024508 (2009).

[35] J. K. Dong, S. Y. Zhou, T. Y. Guan, X. Qiu, C. Zhang, P. Cheng, L. Fang, H. H. Wen, and S. Y. Li, Phys. Rev. B **81**, 094520 (2010).

[36] R. T. Gordon, C. Martin, H. Kim, N. Ni, M. A. Tanatar, J. Schmalian, I. I. Mazin, S. L. Bud'ko, P. C. Canfield, and R. Prozorov, Phys. Rev. B **79**, 100506(R) (2009).

[37] H. Q. Luo, Z. S. Wang, H. Yang, P. Cheng, X. Y. Zhu, and H.-H. Wen, Supercond. Sci. Technol. **21**, 125014 (2008).

[38] G. Mu, H. Luo, Z. S. Wang, L. Shan, C. Ren, and H.-H. Wen, Phys. Rev. B **79**, 174501 (2009).

[39] P. J. Turner, D. M. Broun, S. Kamal, M. E. Hayden, J. S. Bobowski, R. Harris, D. C. Morgan, J. S. Preston, D. A. Bonn, and W. N. Hardy, Rev. Sci. Instrum. **75**, 124 (2004).

[40] A. Hosseini, R. Harris, S. Kamal, P. Dosanjh, J. Preston, R. Liang, W. N. Hardy, and D. A. Bonn, Phys. Rev. B **60**, 1349 (1999).

[41] C. P. Bidinosti and W. N. Hardy, Rev. Sci. Instrum. **71**, 3816 (2000).

[42] H. Chen, Y. Ren, Y. Qiu, W. Bao, R. H. Liu, G. Wu, T. Wu, Y. L. Xie, X. F. Wang, Q. Huang, and X. H. Chen, EPL **85**, 17006 (2009).

[43] J.-H. Chu, J. G. Analytis, C. Kucharczyk, and I. R. Fisher, Phys. Rev. B **79**, 014506 (2009).

[44] G. Li, W. Z. Hu, J. Dong, Z. Li, P. Zheng, G. F. Chen, J. L. Luo, and N. L. Wang, Phys. Rev. Lett. **101**, 107004 (2008).

[45] S. Kamal, R. Liang, A. Hosseini, D. A. Bonn, and W. N. Hardy, Phys. Rev. B **58**, R8933 (1998).

[46] R. Prozorov, M. A. Tanatar, R. T. Gordon, C. Martin, H. Kim, V. G. Kogan, N. Ni, M. E. Tillman, S. L. Bud'ko, and P. C. Canfield, Physica C **469**, 582 (2009).

[47] C. Martin, R. T. Gordon, M. A. Tanatar, H. Kim, N. Ni, S. L. Bud'ko, P. C. Canfield, H. Luo, H. H. Wen, Z. Wang, A. B. Vorontsov, V. G. Kogan, and R. Prozorov, Phys. Rev. B **80**, 020501 (2009).

[48] B. Mühlschlegel, Z. Phys. **155**, 313 (1959).

[49] J. Lee and T. R. Lemberger, Appl. Phys. Lett. **62**, 2419 (1993).

[50] D. A. Bonn, R. Liang, T. M. Riseman, D. J. Baar, D. C. Morgan, K. Zhang, P. Dosanjh, T. L. Duty, A. MacFarlane, G. D. Morris, J. H. Brewer, W. N. Hardy, C. Kallin, and A. J. Berlinsky, Phys. Rev. B **47**, 11314 (1993).

[51] Y. Bang, H. Y. Choi, and H. Won, Phys. Rev. B **79**, 054529 (2009').

[52] M.-S. Kim, J. A. Skinta, T. R. Lemberger, W. N. Kang, H.-J. Kim, E. M. Choi, and S.-I. Lee, Phys. Rev. B **66**, 064511 (2002).

[53] J.-J. Chang and D. J. Scalapino, Phys. Rev. B **40**, 4299 (1989).

[54] A. J. Berlinsky, C. Kallin, G. Rose, and A. C. Shi, Phys. Rev. B **48**, 4074 (1993).

[55] P. J. Turner, R. Harris, S. Kamal, M. E. Hayden, D. M. Broun, D. C. Morgan, A. Hosseini, P. Dosanjh, G. K. Mullins, J. S. Preston, R. Liang, D. A. Bonn, and W. N. Hardy, Phys. Rev. Lett. **90**, 237005 (2003).

[56] D. A. Bonn and W. N. Hardy, in *Physical Properties of High Temperature Superconductors*, edited by D. M. Ginsberg (World Scientific, Singapore, 1996).

[57] R. Harris, P. J. Turner, S. Kamal, A. R. Hosseini, P. Dosanjh, G. K. Mullins, J. S. Bobowski, C. P. Bidinosti, D. M. Broun, R. Liang, W. N. Hardy, and D. A. Bonn, Phys. Rev. B **74**, 104508 (2006).

[58] D. A. Bonn, S. Kamal, K. Zhang, R. Liang, D. J. Baar, E. Klein, and W. N. Hardy, Phys. Rev. B **50**, 4051 (1994).

[59] K. Holczer, L. Forro, L. Mihály, and G. Grüner, Phys. Rev. Lett. **67**, 152 (1991).

[60] N. E. Glass and W. F. Hall, Phys. Rev. B **44**, 4495 (1991).

[61] O. Klein, K. Holczer, and G. Grüner, Phys. Rev. Lett. **68**, 2407 (1992).

[62] H. K. Olsson and R. H. Koch, Phys. Rev. Lett. **68**, 2406 (1992).